Scientific Research Publishing

Open Journal of Inorganic Non-metallic Materials, 2018, 8, 1-10
http://www.scirp.org/journal/ojinm
ISSN Online: 2164-6805
ISSN Print: 2164-6791

# Removal of Aniline Blue from Aqueous Solutions Using $Ce_{1-x}Bi_xCrO_3$ (x = 0, 0.5, 1)

**Labib A. Awin[1*], Mahmoud A. El-Rais[1], Abdunnaser M. Etorki[1], Najat A. Mohamed[2], Wesal A. Makhlof[1]**

[1]Department of Chemistry, Faculty of Science, University of Tripoli, Tripoli, Libya
[2]Department of Chemistry, School of Basic Sciences, Libyan Academy, Tripoli, Libya
Email: *L.Awin@uot.edu.ly, a.etorki@uot.edu.ly

**How to cite this paper:** Awin, L.A., El-Rais, M.A., Etorki, A.M., Mohamed, N.A. and Makhlof, W.A. (2018) Removal of Aniline Blue from Aqueous Solutions Using $Ce_{1-x}Bi_xCrO_3$ (x = 0, 0.5, 1). *Open Journal of Inorganic Non-metallic Materials*, **8**, 1-10.
https://doi.org/10.4236/ojinm.2018.81001

**Received:** November 27, 2017
**Accepted:** January 9, 2018
**Published:** January 12, 2018



## Abstract

The removal of aniline blue dye from aqueous solutions using the *A*-site doped perovskite $Ce_{1-x}Bi_xCrO_3$ (x = 0, 0.5, 1) was investigated. The perovskite oxides were synthesised using Sol-Gel method and characterised by conventional powder X-ray diffraction technique. The X-ray diffraction measurements suggested that doping with Bismuth Ion influences both the crystal structure and the particle size of the oxides, and consequently affects the adsorption properties. It was found that both $CeCrO_3$ and $Ce_{0.5}Bi_{0.5}CrO_3$ compounds are orthorhombic and have approximate particle size of 87 and 36 nm respectively, whereas $BiCrO_3$ oxide has rhombohedral space group symmetry and the particle sizes are less than 49 nm. The batch mode study demonstrated that the removal capacities of Aniline Blue at 150 min and pH = 4.3 for $Ce_{0.5}Bi_{0.5}CrO_3$, $CeCrO_3$ and $BiCrO_3$ are 779.67, 705.45 and 440.18 mg/g respectively. The results reflect the influence of the *A* site doping on the adsorption properties of the oxides. The removal of Aniline Blue was found to be negatively correlated with temperature and pH.

## Keywords

Removal, Aniline Blue, Perovskite Oxides

## 1. Introduction

The residual dyes from textile and printing industries are considered a wide variety of organic pollutants introduced into the water resources. There are ten thousand types of textile dyes with an estimated annual production of seven hundred thousand metric tonnes commercially available worldwide. Thirty percent of these dyes are used more than one thousand tonnes per year, and ninety

percent of the textile products are used at the level of one hundred tonnes per year approximately. About 10% - 25% of textile dyes are lost during the dyeing process whilst 2% - 20% of them are directly discharged as aqueous effluents in different environmental components [1] [2].

The discharge of dye-containing effluents into the wastewater system is undesirable since many of these are toxic, mutagenic and/or carcinogenic to living beings [3]. Furthermore, they affect biodegradation, light penetration and photosynthesis producing imbalance in the ecosystem. For instances, methylene blue, organic dye usually used in cotton and wool manufacturing, can cause serious health problems for human such as vomiting, hard breathing and mental disorder. The absence of effective treatments results in sustaining some components in the environment for a long period. For instance, the half-life of hydrolysed Reactive Blue-19 is ~46 years at pH = 7 and 25˚C [4]. Consequently, treatment methods such as filtration, chemical precipitation, electrolysis, sedimentation, oxidation, photo degradation and adsorption are essentially required.

Adsorption is found to be superior compared to the other methods in term of initial cost, simplicity of construction and insensitivity of toxics. Thus, a wide variety of natural and synthetic materials such as activated carbon, peat, various silica, activated clay, banana pith, natural manganese mineral, oil ash, goat hair, alum sludge, natural zeolite, mixtures of flash, soil and semiconducting oxides have been investigated as dye adsorbents. Among semiconducting oxides, Perovskite type oxides have been proven to be interest due to their efficiency in adsorbing and degrading recalcitrant organic compounds [5].

Perovskite type oxides with the general formula $ABO_3$ have been the focus of numerous studies. The major interest in such materials typically stems from their potential applications in the modern chemical industry such as catalysts, sensors and optical devices [6]. The Perovskite type oxides exist in a variety of compositions and structures each associated with unique physical properties. They contain two different cations, each surrounded by oxygen anion. The larger cation which can be alkali, alkaline earth, or rare earth has, ideally, dodecahedral symmetry, whilst the smaller cation which can be a transition metal ion, is six coordinate. Perovskite can accommodate different combinations of cations, so long as the crystal charge is neutral [7].

This work investigates the removal of Aniline blue (AB) from aqueous solutions using the *A*-site doped perovskite $Ce_{1-x}BixCrO_3$ (x = 0, 0.5, 1). The impact of the replacing of $Ce^{3+}(4f1)$ with $Bi^{3+}(6s2)$ has been addressed to establish the role of the *A*-site cation in controlling the adsorption properties of the oxides. The incorporation of a cation with a stereo chemically active lone pair of electrons onto the *A*-site is known to have a significant effect on the structure and properties of perovskite. This has been explored in the double perovskite $Bi_2FeMoO_6$. It is postulated that the $6s2$ electrons from the $Bi^{3+}$ ions influences the structure and properties [8].

Aniline Blue is typically organic soluble compound utilized in textile industry for dyeing of nylon, wool, silk and cotton. It belongs to triphenyl methane class

of dyeing which a central carbon atom is bonded to two benzene rings and one *p*-quinoid group. Aniline Blue is acidic dye and has long residence time in water [9]. Thus, the presence of such pollutant in industrial discharge water is considered to have numerous impacts on the environment. The removal of industrial dyes from wastewater is a crucial process, from both economic and environmental points of view. It is thought that employing mixed metal oxides such as $Ce_{1-x}Bi_xCrO_3$ in removal of organic dyes can be a good replacement with other high cost adsorbents due to its high accessibility and low cost.

## 2. Experimental

### 2.1. Sample Preparation

To prepare the samples studied in this work the Sol-Gel method was utilized. Appropriate amounts of $Ce(NO_3)_3{\cdot}6H_2O$ (99.9%, BDH), $Cr(NO_3)_3{\cdot}6H_2O$ (99.9%, MERCK) and $Bi(NO_3)_3$ (99.9%, MERCK) were mixed and dissolved in 25 ml of 0.1 M nitric acid (65%, CODEX). The mixture was then added to a citric acid solution (99.7%, BDH) in the mole ratio 1:2 (oxide/acid) and heated on a hotplate at 200˚C until the gel turned ashes. The final products were ground using a mortar and pestle techniques and heated in an alumina crucible within a commercial furnace at 250˚C for 12 hrs and then reground and heated in stages at 400˚C for 12 hrs and 800˚C for 48 hrs.

### 2.2. Instrumentations

The phase composition and purity of the samples was determined from X-ray diffraction. The X-ray diffractometer used was Philips PW 1800 X-Ray generator located at the Libyan Oil institution, Tripoli, Libya with a copper tube (Cu-K$\alpha_1$ radiation), having a wavelength of 1.5406 Å. The operating voltage was 40 kV and the current was 30 mA. The samples were measured in flat plate mode at room temperature with a scan range of $10^\circ < 2\theta < 80^\circ$ and a scan length of 10 mins were used. Diffraction patterns obtained from the Inorganic Crystal Structure Database (ICSD) were used for the comparison with obtained products.

The absorbance of solutions was determined using ultraviolet visible spectrophotometer (UV/V is, model Spect-21D) and (190 - 900 Perkin-Elmer) at maximum wavelength of absorbance (580 nλ). The concentrations of solutions were estimated from the concentration dependence of absorbance fit. The pH measurements were carried out on a WTW720 pH meter model CT16 2AA (LTD Dover Kent, UK) and equipped with a combined glass electrode.

### 2.3. Batch Mode

Batch mode removal studies were carried out by varying several parameters such as contact time, pH, temperature and mass of prepared oxide (adsorbent). Essentially, a 50 ml of dye solution with concentration of 50 ppm was taken in a 250 ml conical flask in which the initial pH was adjusted using HCl/NaOH. Optimized amount of adsorbent was added to the solution and stirred using mag-

netic stirrer for specific time.

## 3. Result and Discussions

### 3.1. Characterization of Oxides

The heating regime described above produced crystalline, green coloured samples. X-ray diffraction measurements showed the $Ce_{0.5}Bi_{0.5}CrO_3$ oxide was isostructural with undoped $CeCrO_3$ and have an orthorhombic (*Pnma*) structure whereas the $BiCrO_3$ oxide has defected rhombohedra perovskite-type structure in space group *R*3*C*. Figure 1 illustrates the XRD patterns of the three oxides calcined at 800˚C. The Average Crystallite size $D_p$, Line broadening in radians $\beta$, Bragg angle $\theta$, X-ray wavelength $\lambda$ and lattice strain estimated from X-ray diffraction data are summarised in Table 1.

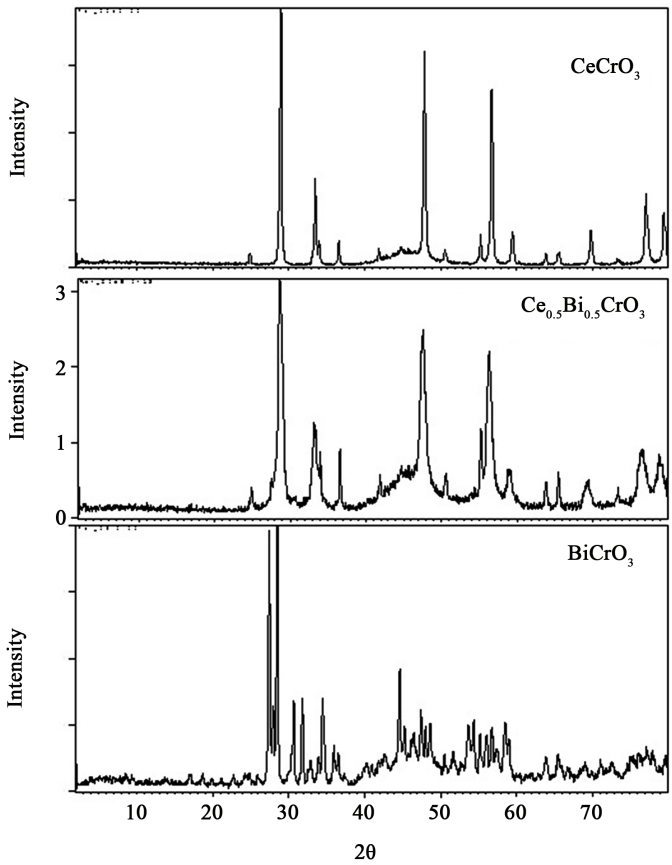


Figure 1. XRD patterns of $CeCrO_3$, $Ce_{0.5}Bi_{0.5}CrO_3$ and $BiCrO_3$ calcined at 800˚C.

Table 1. Average crystallite size $D_p$, Line broadening in radians $\beta$, Bragg angle $\theta$, X-ray wavelength $\lambda$, lattice strain estimated from X-ray diffraction data.

| Oxide | $\lambda$ (Å) | $\theta$ (˚) | $\beta$ | $D_p$ (nm) | Lattice strain |
|---|---|---|---|---|---|
| $CeCrO_3$ | 1.54056 | 29.023 | 0.0984 | 87.14 | 0.0017 |
| $Ce_{0.5}Bi_{0.5}CrO_3$ | 1.54056 | 28.559 | 0.2362 | 36.26 | 0.0040 |
| $BiCrO_3$ | 1.54056 | 28.537 | 0.1771 | 48.36 | 0.0030 |

The crystallite size can be calculated using sheerer formula [10]:

$$D_p = 0.94\lambda/\left(\beta_{1/2}\cos\theta\right)$$

Unexpectedly, $Ce_{0.5}Bi_{0.5}CrO_3$ displayed the lowest crystallite size, whereas the $CeCrO_3$ had the highest crystallite size in the series. The decrease in crystallite size of $Ce_{0.5}Bi_{0.5}CrO_3$ and $BiCrO_3$ is inconsistent with the relative ionic size of the $Bi^{3+}$ (8 coordinate ionic radius, 1.17 Å) and $Ce^{3+}$ (1.14 Å) cations [11]. The decrease in crystallite size of Bi doped oxides can be attributed to the high covalent bonding character of Bi ions, with small displacement of the *A*-site cations enhanced by the covalence [12] [13].

## 3.2. Batch Mode

### 3.2.1. Effect of Contact Time

The removal percentage of dyes over the adsorbents can be calculated as:

$$R\% = \left[\left(C_i - C_t\right)/C_i\right]\times 100$$

where $R\%$ is the removal percentage, $C_i$ = 50 ppm is initial concentration of dye solutions, $C_t$ is the concentration of dye at contact time estimated from the concentration dependence of absorbance fit. The effect of contact time on the AB removal was observed at the range of (0 - 150 min). **Figure 2** shows the time dependence of AB removal at room temperature. There is no finite time was observed for the dye removal up to 150 min. The removal of dye increases as the contact time increased. The removal of AB on the surface of $CeCrO_3$, $Ce_{0.5}Bi_{0.5}CrO_3$ and $BiCrO_3$ at 150 min were found to be 58.30%, 59.25% and 41.72% respectively.

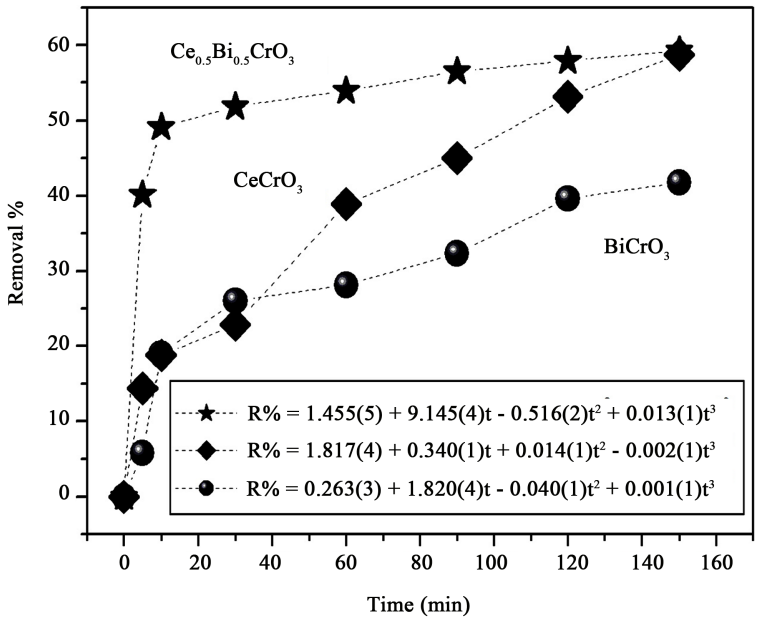


**Figure 2.** Time dependence of AB removal at room temperature. The volume, concentration and pH of the AB solution are 50 ml, 50 ppm and 4.3 respectively. The time dependent variation of the removal is fitted as labelled on the figure.

### 3.2.2. Effect of Adsorbent Mass

The amount of the dye adsorbed by one gram of the oxides ($Q$) was calculated as following:

$$Q(\mathrm{mg/g}) = \left[\left(C_i - C_t\right) \times V\right] / W$$

where $t$ = 150 min is the contact time, $V$ = 50 ml is the volume of AB solution and $W$ is the mass of oxides. As shown in Figure 3, $Q$ decreases as the mass of adsorbents increased. The maximum capacity of adsorbent $Q_{max}$ can be estimated from the intercept of the liner fit of $1/Q_t$ at Y axis. $Ce_{0.5}Bi_{0.5}CrO_3$ displayed the highest value of $Q_{max}$ (779.67 (6) mg/g) whereas $BiCrO_3$ exhibited the lowest value of $Q_{max}$ (440.18 (4) mg/g). $Q_{max}$ for $CeCrO_3$ is 705.45 (1) mg/g. This result reflects the importance of the element composition and crystal structure of the oxides. The amount of AB adsorbed by $CeCrO_3$ which has orthorhombic lattice and the largest crystallite size (87.14 nm) is much higher than that adsorbed by $BiCrO_3$ which has rhombohedral lattice and crystallite size equal to 48.36 nm. The observed increase in the removal using $Ce_{0.5}Bi_{0.5}CrO_3$ which has orthorhombic lattice and the smallest crystallite size (36.26 nm) suggested an enhancement in the adsorption properties occurs as result of the substitution of $Bi^{3+}$ into the oxide plus the decrease in crystallite size. The decrease in crystallite size leads to an increase in the surface area of particles.

### 3.2.3. Effect of pH

To study the effect of pH, experiments were carried out at various pH values, ranging from 2 to 6 for constant dye concentration (50 ppm) and adsorbent mass (0.1 g). Figure 4 shows the removal of AB as a function of pH. The removal of AB increases as pH decreased. The highest removal of AB for $CeCrO_3$,

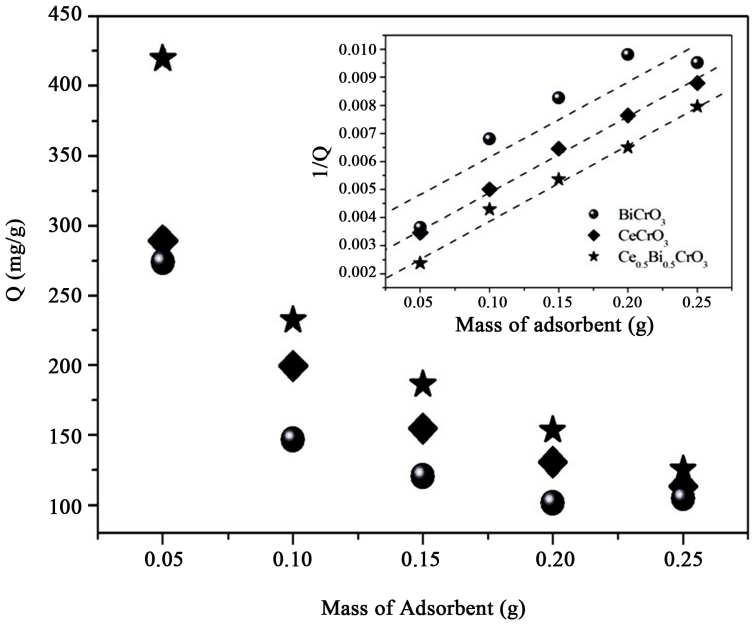


Figure 3. Effect of mass adsorbent on the removal. The time, volume, concentration and pH of the AB solution are 150 min, 50 ml, 50 ppm and 4.3 respectively.

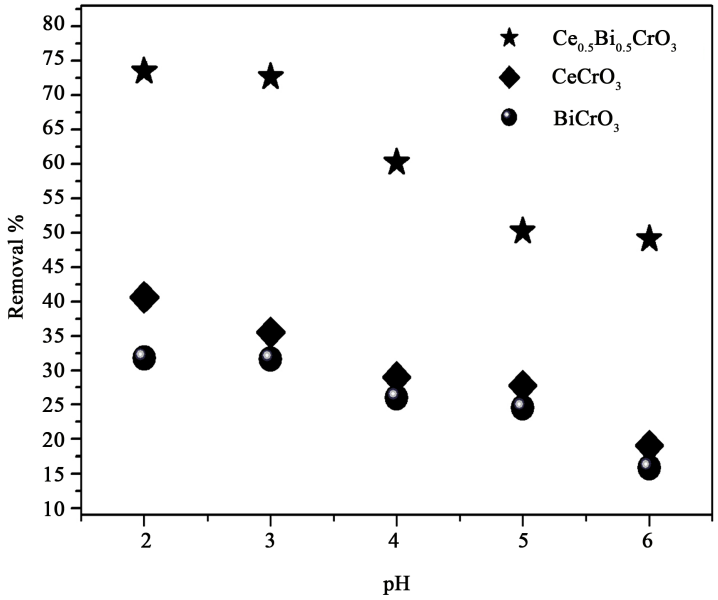


**Figure 4.** Effect of pH on the removal of AB. The time, volume and concentration of the AB solution are 150 min, 50 ml and 50 ppm respectively.

$Ce_{0.5}Bi_{0.5}CrO_3$ and $BiCrO_3$ are found to be 87.36%, 86.00%, 81.28% respectively at pH = 2. The oxides displayed almost an equal efficiency of removal (~53%) at pH = 6. $BiCrO_3$ exhibited lower percentages of removal compare to the two other oxides. The interpretation of pH effects on the efficiency of the adsorption process is a very difficult task, because of its multiple roles. It is related to the acid base property of both the metal oxide and the organic dye. The adsorption of water molecules at metal sites is followed by the dissociation of $OH^-$ groups, leading to coverage with chemically equivalent metal hydroxyl groups (M-OH). Due to amphoteric behaviour of both the metal oxide and the organic dye, the equilibrium reactions below are considered. The electrostatic interactions between the positive catalyst surface and dye anions leading to strong adsorption of the last on the oxide support.

1) $M-OH + H^+ \leftrightarrow M-OH_2^+$
2) $M-OH \leftrightarrow M-O^- + H^+$
3) $Dye-OH + H^+ \leftrightarrow Dye^+ + H_2O$
4) $H-Dye + OH^- \leftrightarrow Dye^- + H_2O$

### 3.2.4. Effect of Temperature

Temperature has an important impact on the adsorption process. An increase in temperature helps the reaction to compete more efficiently with $e^-/H^+$ recombination. The removal of AB was investigated at 25˚C, 40˚C, 60˚C and 100˚C. The obtained results are illustrated below in **Figure 5**. The removal of AB decreased as temperature increased. For instance, the removal of AB using $Ce_{0.5}Bi_{0.5}CrO_3$ decreased from 61.44% at 25˚C to 30.06% at 100˚C. The decrease in percentages of adsorption with rise in temperature may be due to desorption caused by an increase in the thermal energy. Higher temperature induces higher mobility of

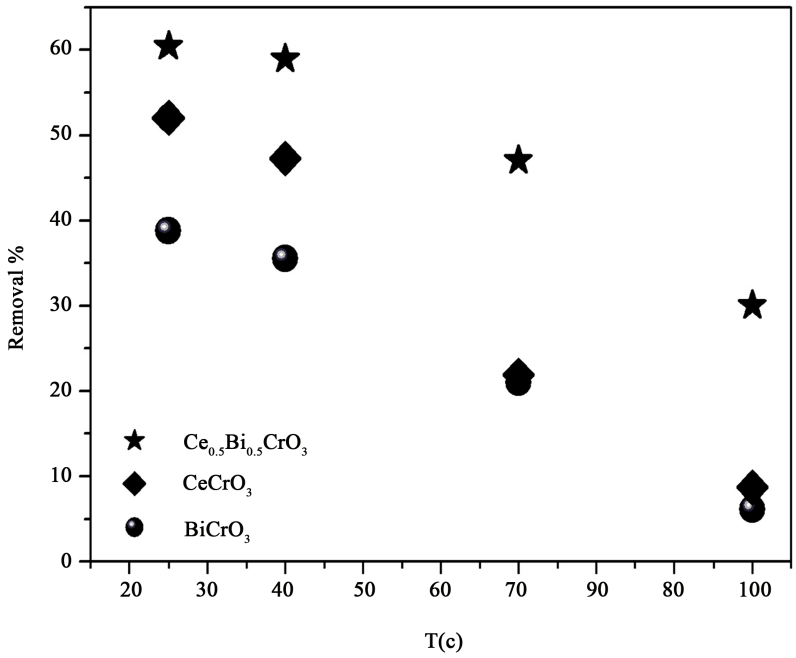


**Figure 5.** Effect of temperature on the removal of AB. The time, volume and concentration of the AB solution are 150 min, 50 ml and 50 ppm respectively.

active sites of adsorbents and the surface area is decreased by increase the temperature.

The energy of activation ($E_a$), was calculated from the Arrhenius plot of ln$R$ vs 1000/$T$ (**Figure 6**). Arrhenius plot shows that the activation energies of the removal of AB using $CeCrO_3$, $Ce_{0.5}Bi_{0.5}CrO_3$ and $BiCrO_3$ are negative and equal to −22.58 ± 1, −8.53 ± 1 and −22.21 ± 1 kJ·mol$^{-1}$ respectively. This result is contrary to normal expectations, and is a consequence of the competition between two effects: the increase of intrinsic kinetics with temperature, and the decrease of adsorption strength and the concentration of active intermediates with temperature [14]. The adsorption of AB dye can be described as barrierless reaction, in which the reaction proceeding relies on the capture of the molecules in a potential well. Increasing the temperature leads to a reduced probability of the colliding molecules capturing one another (with more glancing collisions not leading to reaction as the higher momentum carries the colliding particles out of the potential well), expressed as a reaction cross section that decreases with increasing temperature. Such a situation no longer leads itself to direct interpretations as the height of a potential spot [15].

## 4. Conclusion

The removal of Aniline blue from aqueous solution by the mixed metal perovskite $Ce_{1-x}Bi_xCrO_3$ has been studied. In general, the amount of AB adsorbed by $Ce_{0.5}Bi_{0.5}CrO_3$ is higher than those adsorbed by $CeCrO_3$ and $BiCrO_3$. The study showed no finite time for the AB removal up to 150 min. The AB removal increases as the mass of the oxides increases. The adsorption of AB was

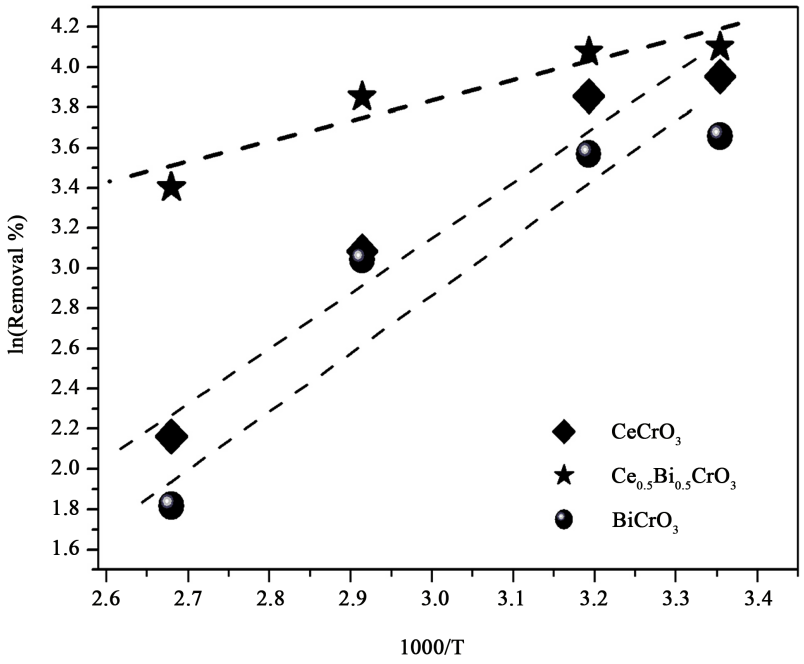


**Figure 6.** Arrhenius plot of ln(Removal %) vs 1000/T($K^{-}$).

temperature and pH dependent. The three oxides showed maximum removal efficiency of AB at 25˚C and pH = 2.0. The adsorption capacity of AB from water was 779.67, 705.45 and 440.18 mg/g using $Ce_{0.5}Bi_{0.5}CrO_3$, $CeCrO_3$ and $BiCrO_3$ respectively. The study indicated that doping with Bismuth ions into $CeCrO_3$ can successfully enhance the adsorption properties of the oxide.

## Acknowledgements

Authors thank the Libyan Oil institution for the XRD measurements. Many thanks for Prof. Abd El-Salam. M. Elmehob for the paper proofreading.

## References

[1] Baban, A., Yediler, A. and Ciliz, N.K. (2010) Integrated Water Management and CP Implementation for Wool and Textile Blend Processes. *CLEAN—Soil, Air, Water*, **38**, 84-90. https://doi.org/10.1002/clen.200900102

[2] Robinson, T., McMullan, G., Marchant, R. and Nigam, P. (2001) Remediation of Dyes in Textile Effluent: A Critical Review on Current Treatment Technologies with a Proposed Alternative. *Bioresource Technology*, **77**, 247-255. https://doi.org/10.1016/S0960-8524(00)00080-8

[3] Carmen, Z. (2012) Textile Organic Dyes—Characteristics, Polluting Effects and Separation/Elimination Procedures from Industrial Effluents—A Critical Overview. InTech, Janeza Trdine Rijeka, Croatia.

[4] Hao, O.J., Kim, H. and Chiang, P.-C. (2000) Decolorization of Wastewater. *Critical Reviews in Environmental Science and Technology*, **30**, 449-505. https://doi.org/10.1080/10643380091184237

[5] Ruthven, D.M. (1984) Principles of Adsorption and Adsorption Processes. Wiley, Hoboken, NJ.

[6] Wong-Ng W.K., Goyal, A., Guo, R. and Bhalla, A.S. (2012) Synthesis, Properties, and Crystal Chemistry of Perovskite-Based Materials. Wiley, Hoboken, NJ.

[7] Ishihara, T. (2009) Structure and Properties of Perovskite Oxides. In: *Perovskite Oxide for Solid Oxide Fuel Cells*, Springer, Berlin, Germany.

[8] Lan, Y., Feng, X., Zhang, X., Shen, Y. and Wang, D. (2016) Effects of Bi Doping on Structural and Magnetic Properties of Double Perovskite Oxides $Sr_2FeMoO_6$. *Physics Letters A*, **380**, 2962-2967. https://doi.org/10.1016/j.physleta.2016.06.057

[9] Hofmann, A. (1862) Note on the Composition of Aniline-Blue. *Proceedings of the Royal Society of London* (1854-1905), **12**, 578-579. https://doi.org/10.1098/rspl.1862.0128

[10] Langford, J.I. and Wilson, A.J.C. (1978) Scherrer after Sixty Years: A Survey and Some New Results in the Determination of Crystallite Size. *Journal of Applied Crystallography*, **11**, 102-113. https://doi.org/10.1107/S0021889878012844

[11] Shannon, R.D. (1976) Revised Effective Ionic-Radii and Systematic Studies of Interatomic Distances in Halides and Chalcogenides. *Acta Crystallographica Section A*, **32**, 751-767.

[12] Takagi, S., Subedi, A., Cooper, V.R. and Singh, D.J. (2010) Effect of A-Site Size Difference on Polar Behavior in $MBiScNbO_6$ (M=Na, K, and Rb): Density Functional Calculations. *Physical Review B*, **82**, 134108.

[13] Corker, D.L., Glazer, A.M., Kaminsky, W., Whatmore, R.W., Dec, J. and Roleder, K. (1998) Investigation into the Crystal Structure of the Perovskite Lead Hafnate, $PbHfO_3$. *Acta Crystallographica Section B*, **54**, 18-28. https://doi.org/10.1107/S0108768197009208

[14] Wei, J. (1996) Adsorption and Cracking of N-Alkanes over ZSM-5: Negative Activation Energy of Reaction. *Chemical Engineering Science*, **51**, 2995-2999. https://doi.org/10.1016/0009-2509(96)00187-X

[15] Mozurkewich, M. and Benson, S.W. (1984) Negative Activation Energies and Curved Arrhenius Plots. 1. Theory of Reactions over Potential Wells. *Journal of Physics and Chemistry*, **25**, 6429. https://doi.org/10.1021/j150669a073